

Full Length Article

Seismic performance evaluation of mass timber buildings equipped with resilient and conventional friction devices

Ashkan Hashemi*, Rajnil Lal

Department of Civil and Environmental Engineering, The University of Auckland, New Zealand



ARTICLE INFO

Keywords:

Mass timber
Resilience
Dampers
Friction
Energy dissipation

ABSTRACT

The application of mass timber elements in different structures has gained publicity over the last few years, primarily due to climate change adaptation policies and net zero carbon targets. Timber is a renewable construction material that can outperform other building materials regarding environmental impact. However, when used in seismically active regions, its application has been limited due to the uncertainties on their seismic behaviour in respect with different design standards and limited ductility in conventional connections. Conventional timber connections typically suffer from stiffness and strength degradation under cyclic loads. Their reparability is also low due to permanent damage in the fasteners and the associated crushing in the wood fibres. The use of friction connections can be an efficient way to mitigate these issues. They offer many advantages as they are economical and yet provide a high level of reliable and continuous energy dissipation. In recent years, a new generation of friction connections has been developed that can provide self-centring behaviour (i.e., the ability of the structure to return to its original position at the end of an earthquake). However, how these connections perform compared to a mass timber system with conventional timber connections is still unknown.

Several studies in the literature have suggested that these connections can enhance the performance of mass timber structures. However, the seismic performance of such systems specifically in terms of base shear, response drifts and response accelerations—has not been thoroughly investigated. This paper examines various design aspects of conventional friction connections and self-centring friction connections, providing insights into their differences concerning key seismic performance indicators. It compares the seismic performance of mass timber buildings equipped with both solutions, highlighting their advantages and limitations and drawing conclusions based on the results. The key findings are that friction connections can provide a superior seismic performance for timber structures. However, that may need to be combined with a parallel system avoid residual displacements.

1. Introduction

The application of mass timber elements in various types of structures has gained popularity over the last two decades, primarily due to the industry's shift towards reducing carbon content and the goal of achieving net-zero carbon emissions. Timber is a renewable construction material with significantly lower carbon content compared to other building materials like steel or concrete [1,2]. While there has been a surge of interest in timber buildings, their use in seismically active areas presents challenges. See Fig. 1 as an example of timber braced frames.

Timber's brittle nature (noting that not all failure modes of timber is brittle, but brittle failure modes may govern many cases) means that the required ductility for seismic performance must come from its connections. Research into timber's earthquake performance shows that con-

ventional connections using dowel-type fasteners (such as screws or rivets) may not provide sufficient ductility compared to steel or concrete structures [3–5]. Additionally, damage to these fasteners—necessary to achieve ductility—can be irreversible and may cause crushing of timber fibres. This leaves structures vulnerable to aftershocks and future seismic events even if they withstand the initial quake.

Large-scale testing of structural systems made with massive wooden elements and conventional connectors has highlighted both the strengths and weaknesses of such designs. One of the most comprehensive studies in this area is the SOFIE project [6], which tested full-scale three- and seven-storey specimens on a shake table. While the overall seismic performance of the tested specimens was deemed acceptable, significant and irreparable damage occurred in the connections. Additionally, it was observed that supplementary sources of energy dissipation, such as seismic dampers, might be necessary to mit-

* Corresponding author.

E-mail address: a.hashemi@auckland.ac.nz (A. Hashemi).



Fig. 1. An example of a timber braced frame (the Hive, designed by Fast+Epp consulting, BC, Canada).

igate the high accelerations, which reached up to 3.9 g at the upper floors.

Chen and Popovski et al. [7,8] investigated the seismic response of mass timber systems with different connectors and concluded that the pinching behaviour of connections is the governing mode of failure. Similarly, Gavric et al. [9] studied the seismic performance of single and coupled Cross Laminated Timber (CLT) walls and found that the plastic yielding of the connections dictated the overall system performance, eventually leading to failure.

In a full-scale two-story CLT house tested by Popovski and Gavric [10], the results showed that although the seismic response was acceptable, the drift capacity of the system could be a limiting factor in its performance. Yasumura et al. [11] examined the mechanical characteristics of conventional mass timber systems under reversed cyclic loads and concluded that failure in the connections significantly limits seismic performance. Overall, the studies mentioned above confirmed that failure in timber connections used in lateral load-resisting systems is the primary factor governing their seismic performance. Consequently, damage avoidance and more robust connection designs are necessary to enhance seismic resilience. This has motivated many researchers to initiate new studies exploring the replacement of conventional connections with high-performance, innovative connectors to achieve improved seismic performance [12]. Yan et al. investigated seismic performance of CLT structures with tuned mass dampers made with shape memory alloy [13]. Their findings demonstrated that the seismic performance of such buildings can be improved compared to conventional construction in terms of sustaining stiffness of strength of the system. Badal and Tesfamariam [14] looked into the collapse performance of high-rise mass timber frames with Buckling Restrained Braces. Similarly, the system performed compared to conventional timber buildings given the absence of pinching behaviour in Buckling Restrained Braces. Daneshvar et al. [15] experimentally investigated the performance of mass timber systems with connections made with perforated steel plates. Chen et al. [16] performed a seismic performance evaluation on post-tensioned steel frames with hybrid braces. All these findings demonstrate that when conventional timber connections are replaced with more advanced mechanisms, superior seismic performance can be achieved. The pinching behaviour (loss of stiffness over cycles of loading and unloading) of dowel-type fasteners may cause the building to behave undesirably under cyclic loads. However, the above research projects demonstrate when these connections are replaced with more advanced connections the overall performance of the building can be significantly enhanced. A promising candidate for this replacement is the sliding friction connection, which is the focus of this study. The next section provides further details on this type of connection.

2. Sliding friction connections

Sliding friction connections are widely recognised as one of the most efficient energy dissipation mechanisms due to their economic and performance advantages. These connections dissipate energy through the frictional resistance between two or more plates clamped together with bolts, offering a high rate of energy dissipation and exhibiting behaviour close to an elastic-perfectly-plastic system. Their development dates back to the 1970s when Pall et al. [17,18] introduced and applied them to steel-braced frames and concrete shear wall structures. The tests performed by Pall et al. demonstrated a reliable, non-degrading hysteretic performance that remained independent of velocity.

Building on this, Popov et al. [19] proposed Slotted Bolted Connections (SBCs) for use in steel Moment Resisting Frames (MRFs). Their physical tests revealed significant improvements in performance compared to conventional MRFs with welded beam-column connections. Filiatrault [20] was among the first to test asymmetrical friction joints for traditional timber walls. These tests involved friction connections at the corners of each wall panel, demonstrating a superior load-deformation performance compared to traditional timber walls with standard studs.

Through experimental investigations, Bora et al. [11] explored the use of slip friction connections in rocking precast concrete walls, while Loo et al. [21] became pioneers in applying a similar concept to mass timber structures. Their cyclic tests on a rocking Laminated Veneer Lumber (LVL) wall system showed a reliable hysteretic performance, successfully avoiding the pinching effect (a common issue in conventional mass timber systems) through the use of slip friction hold-downs. Dal Lago et al. [22] also investigated the application of sliding friction connections for structures with precast concrete walls, contributing to the growing body of research demonstrating the effectiveness of these devices.

Overall, the introduction and application of sliding friction connections in concrete, steel, and timber structures have proven to be a reliable solution for enhancing seismic performance by mitigating degradation, improving energy dissipation, and addressing the vulnerabilities of conventional connections. These devices offer a load-deformation behaviour similar to an elastic-perfectly plastic system, often referred to as “fat hysteresis” [23]. This type of hysteresis provides a high rate of energy dissipation, which may be useful for seismic design.

However, while this system excels in dissipating energy, it has a potential drawback: the tendency to develop significant residual displacements. After a seismic event, a large force might be required to return the structure to its original position once the sliding friction connections are activated. This residual displacement can be problematic, as it may leave the structure with permanent deformations that make it susceptible to future seismic events or even lead to its demolition despite surviving the initial earthquake.

Research has shown that residual displacements can present a significant challenge in post-earthquake scenarios, as the structure may remain misaligned or damaged [24,25]. This highlights the importance of exploring alternative friction connection designs, such as those with self-centring capabilities, to avoid such permanent deformations while maintaining efficient energy dissipation [26,27]. To address this issue, a new generation of technology called the Resilient Slip Friction Joint (RSFJ) [28] has been introduced. This device provides both damping and self-centring capabilities in one package, significantly improving it over traditional sliding friction connections.

Fig. 2 illustrates the components and the expected load-deformation behaviour of the RSFJ. The device consists of profiled ridged plates clamped together using semi-compressed stacks of disc springs. When the device is loaded, the frictional resistance between the moving orange plates is overcome, causing the semi-compressed stacks of springs to become further compressed until they are fully flattened. At this point, the device reaches its maximum strength (commonly referred to as F_{ult}). Upon unloading, the energy stored in the springs returns the orange

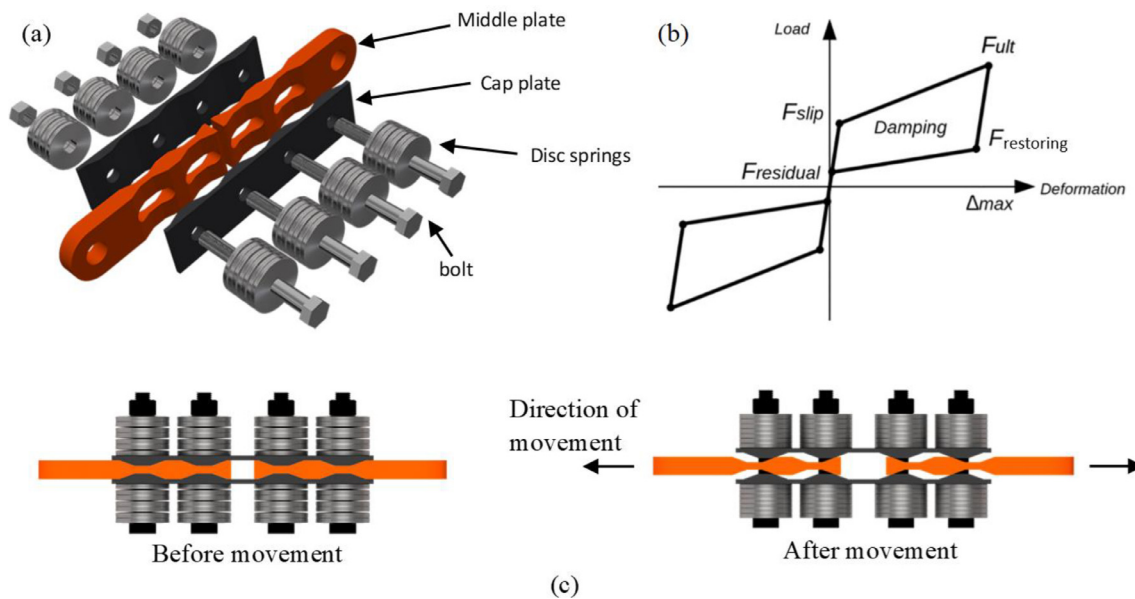


Fig. 2. RSFJ (a) components (b) hysteresis (c) at rest and expansion [29].

sliding plates to their original position. This same performance is expected under compressive loading, resulting in the characteristic load-deformation behaviour depicted in Fig. 2(b). For a more detailed explanation of the device's performance and component test results, readers are referred to [28] which delve into the RSFJ's technical specifications and testing outcomes. Note that it assumed the plates of the RSFJ device are designed in a way that it is not possible that they jump between the corrugations (from one groove to another). In other words, the device will reach its maximum design displacement before this happens [29].

The introduction of the RSFJ represents a promising solution to address the shortcomings of traditional sliding friction connections by offering a robust self-centring mechanism, improving both the performance and resilience of structures in seismic events. This technology and its applications have been the subject of numerous research projects. Hashemi et al. investigated the use of the RSFJ device as hold-down connectors for mass timber rocking walls and columns [30], demonstrating its effectiveness in these applications. Yousef-Beik et al. [31] showcased the device's value for diagonal tension-compression braces, while Bagheri et al. [32] experimentally examined its use in ductile tension-only connections. Given the unique benefits the RSFJ technology offers, it has been adopted in several real-world projects (refer to [33] and [34] for some example projects), where its ability to enhance both energy dissipation and resilience has proven critical for structural performance, particularly in seismic-prone areas [33].

As mentioned in Section 1, several different structural systems have been used to design multi-storey mass timber buildings in seismic-prone areas. However, there is still significant scope to investigate which system is best, especially if resilience is prioritised over the minimum design requirement (which focuses solely on life safety). Although the RSFJ technology has been tested and studied for various applications, less attention has been paid to investigating the behaviour of the entire building as a system.

In one of the few studies that explored this issue, Hashemi et al. [35] examined the behaviour of mass timber buildings equipped with rocking CLT walls and RSFJ hold-downs in comparison to conventional slip friction connections and nailplates. They concluded that self-centring hold-downs outperformed the other two structural systems in terms of response drifts, response accelerations, and base shear. Although wall systems with conventional slip friction connections often performed bet-

Table 1
Structural systems investigated.

System code	Type of LLRS	Number of Storeys
R1	RBF	2
R2	RBF	6
R3	RBF	12
S1	SFBF	2
S2	SFBF	6
S3	SFBF	12
D1	Dual system with SFBF and MRF	2
D2	Dual system with SFBF and MRF	6
D3	Dual system with SFBF and MRF	12

ter in terms of energy dissipation, the risk of large residual displacements increased significantly.

This study conducted a comprehensive investigation into the seismic performance of mass timber buildings equipped with Slip Friction Braced Frames (SFBFs) and RSFJ Brace Frames (RBFs). To ensure thoroughness, a comprehensive analysis matrix has been developed. As shown in Table 1, three main systems are considered: Structural systems with RBFs as the primary Lateral Load Resisting System (LLRS), Structural systems with SFBFs as the primary LLRS and Structural systems with a dual LLRS consisting of SFBFs and backup Moment Resisting Frames (MRFs). The rationale for including the dual LLRS is based on standards like ASCE-7 [36], which recommend using energy dissipation systems in a dual configuration. Although these standards do not explicitly address friction dampers, they have been included in this study to allow a comparison with structural systems where friction-damped braces are the sole LLRS.

For each LLRS, three models are analysed for two-storey, six-storey, and twelve-storey frames to assess the effect of height and stiffness on overall seismic performance. These building types were selected to represent low- mid- and high-rise frames respecting the New Zealand building industry. For simplicity, the systems with RBFs as the main LLRS are named R1 to R3, the systems with SFBFs as the main LLRS are named S1 to S3, and the systems with dual LLRS are named D1 to D3. Table 1 summarises the models under consideration. Note that none of the current studies in the literature directly compared the most important seismic performance indexes shown in Table 1 and this study for the first time makes this comparison and provides design insights for researchers and

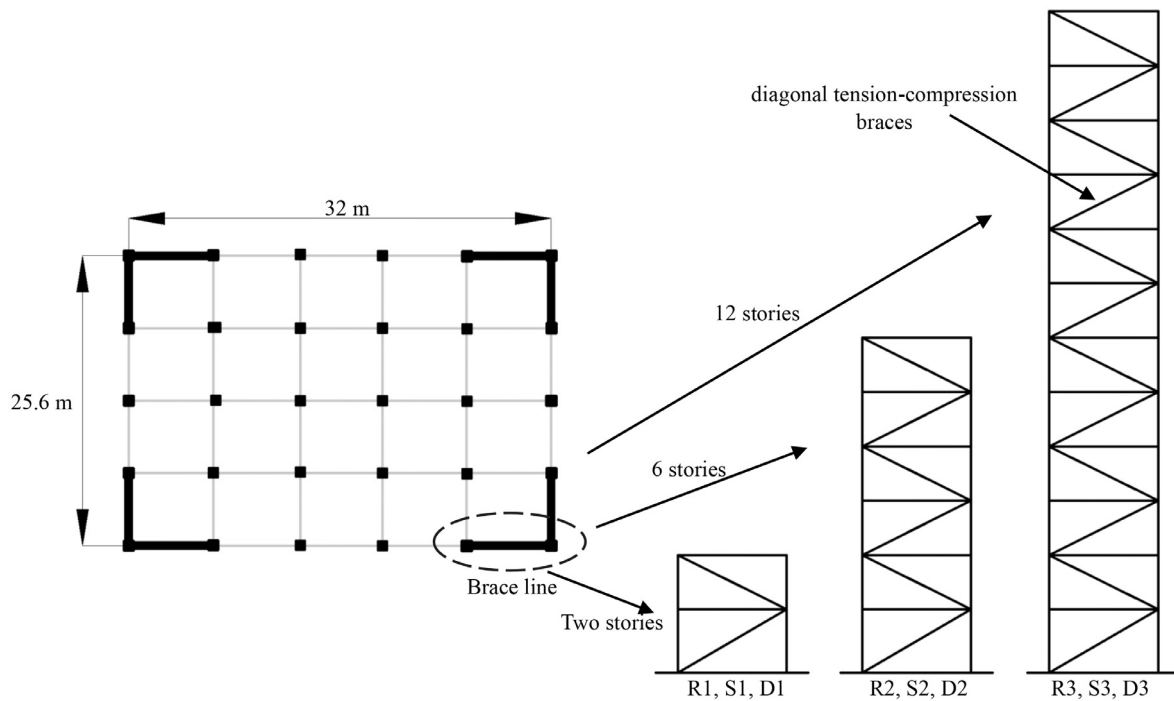


Fig. 3. The general layout of the structure.

engineers. Also note that the friction-damped brace systems used in S1 to S3 and D1 to D3 system is also known as conventional friction damper unit shown in Fig. 4(b).

3. The case study structure and design procedure

A case study was conducted using a prototype architectural plan of a mass timber building located in Christchurch, New Zealand (representing a high seismic zone), to design and evaluate the seismic performance of the various scenarios outlined in Table 1. The building is intended for public use, and as such, an importance level of 3 (representing high-importance building) was assigned in accordance with the New Zealand Standard for Earthquake Actions [37]. As specified in the standard, two design limit states must be considered for seismic design: the Serviceability Limit State (SLS) and the Ultimate Limit State (ULS). The SLS criteria ensure the building can be reoccupied quickly after small to moderate earthquakes, as indicated by the Return Period Factor $R_s=0.25$. The ULS design level actions, on the other hand, are based on a return period factor of $R_u=1.3$. The hazard factor specific to Christchurch is $Z = 0.3$. Furthermore, the structure is assumed to be located on deep or soft soil, categorised as Type D according to the standard.

The inter-storey heights are 3.5 m for the first floor and 3.2 m for the remaining floors, giving the structure a total height of 6.7 m for the R1, S1, and D1 models, 19.5 m for the R2, S2, and D2 models, and 38.7 m for the R3, S3, and D3 models. Timber diagonal braces are used for lateral load resistance, while gravity loads are carried by a frame comprising gravity beams and columns. Fig. 3 shows the building layout, the assumed locations for the brace lines, and the different analysis cases considered, as defined in Table 1.

The permanent dead loads assumed in the design are 1.5 kPa for all floors, covering the weight of key structural elements, interior and exterior walls, ceilings, and light timber flooring. The imposed loads are 2 kPa for the first floor, 1.5 kPa for the second to fifth floors, and 0.5 kPa for the roof. The corresponding seismic masses are 164 tonnes for the first floor, 152 tonnes for all intermediate floors, and 129 tonnes for the roof. Given the building's symmetrical layout, it was assumed

that the seismic load in each direction is evenly distributed among the four brace lines (see Fig. 3). The seismic masses assigned to each brace line are 41 tonnes for the first floor, 38 for all intermediate floors, and 32 for the roof. Although the additional demand on the braces due to accidental eccentricity is not considered in this study for simplicity, it is advisable to include this factor in practice, as it could have a small but noteworthy effect. The braces are assumed to be made from Glulam (glued-laminated timber) elements with a strength grades ranging from 8 to 12 MPa.

4. Design and modelling of the braces

For each of the building archetypes described in the previous section, a numerical model was developed using the ETABS software package [38]. This resulted in nine separate models, all sharing the same architectural plan, to represent the nine different cases outlined in Table 1.

As mentioned, it was assumed that the beams, columns, and braces are constructed using Glulam members with grades ranging from 8.0 to 12.0. Additionally, it was assumed that friction devices are attached to one end of the braces using link elements across all models (see Fig. 5). Fig. 5 illustrates the arrangement of the numerical models, while Table 2 provides the section sizes for beams, braces, and columns. Note that while a diagonal brace arrangement used for this conceptual study, other bracing configurations (e.g. V-braces) might be more efficient for some projects.

For all systems, a ductility factor of 3.0 was assumed for the design. It was previously demonstrated that all investigated systems can be confidently designed with this level of ductility [41,42]. This approach has been adopted to ensure an accurate comparison between the different systems outlined in Table 1. Readers are referred to [41,43] for more detailed information on the design procedures for the self-centring systems, which include a displacement-based design approach to achieve a resilient design.

As mentioned in the previous section, return period factors of $R_s=0.25$ for SLS and $R_u=1.3$ for ULS were adopted. As shown in Fig. 5, the braces were as a link element representing the brace bodies (e.g. GL members) in series with the friction device. Refer to [44] for the details

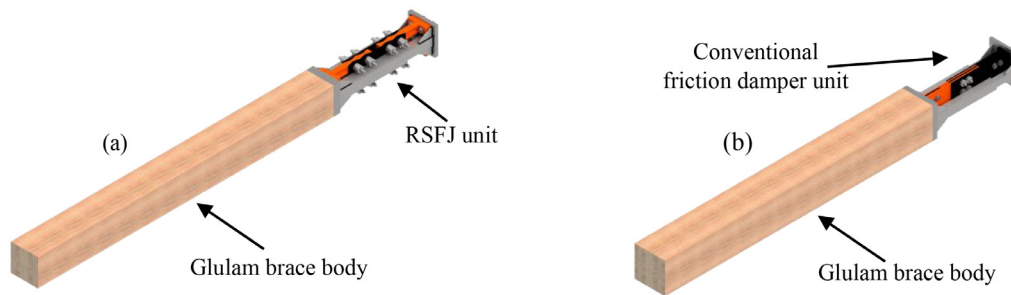


Fig. 4. The general arrangement of the Glulam braces with the friction devices attached: (a) Timber braces with RSFJs [39] (b) Timber braces with conventional friction connections [40].

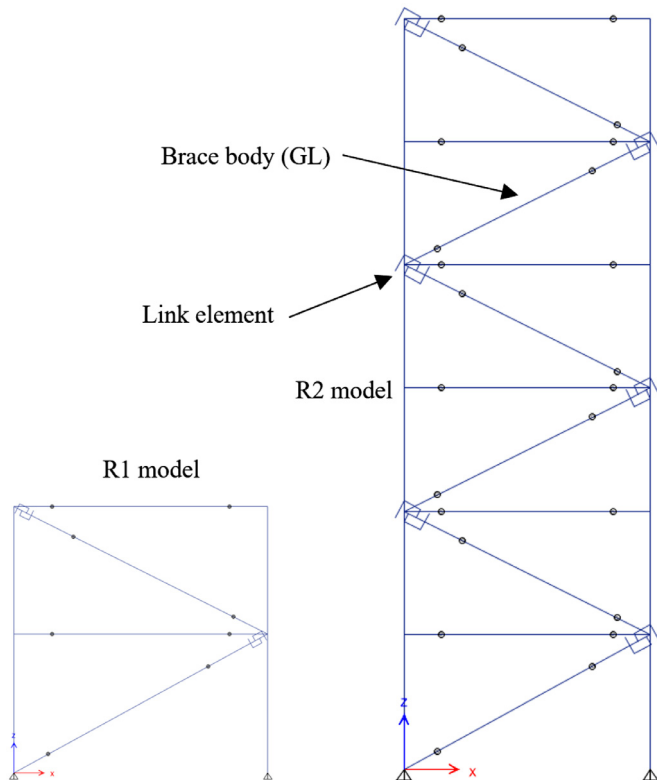


Fig. 5. Examples of the arrangement of the numerical models (two models shown as representative for all).

and verification of this modelling technique. Note that GL sections defined as elastic frame sections in the model). For the RSFJ devices (models R1 to R3), the "Damper–Friction Spring" link element were used. This modelling approach has been validated by the authors through comparing numerical data with experimental results in different forms and arrangements [41]. For further details on the modelling and experimental verification, readers are referred to [45,46–48].

The friction devices in the SFBF systems (models S1 to S3) were modelled using the "Plastic Wen" elements. This hysteretic type can be selected when define a non-linear link element in ETABS. In the dual systems (models D1 to D3), the complementary moment-resisting frames (MRFs) were modelled as rotational springs at the beam-column joints, with stiffness equivalent to 25 % of the stiffness of the braces (inspired by design requirements of dual lateral load resisting systems cited in international standards [36]). Table 3 provides the specifications of the braces used in all nine models.

To verify the modelling and evaluate the performance of each system under cyclic loads, a series of Nonlinear Static Pushover (NSP) anal-

yses was conducted. Fig. 6 presents the results of these analyses, illustrating one cycle of loading and unloading for the structures. As observed, the systems equipped with RSFJ braces (R1 to R3) exhibit a flag-shaped response, confirming that fully self-centring performance has been achieved. The systems with FDBFs as the primary lateral load-resisting mechanism exhibited Elastic-Perfectly-Plastic (E-P-P) behaviour due to the hysteretic response of the braces.

Lastly, the systems incorporating dual lateral load-resisting mechanisms displayed a response akin to E-P-P behaviour but with a positive post-slip stiffness (e.g. the stiffness of the building after the braces are activated). This characteristic can be beneficial in minimising permanent residual displacements (e.g. permanent out-of-straightness of the building at the end of earthquake). Additionally, the results demonstrated that the systems did not exhibit any stiffness or strength degradation, which aligns with the damage-avoidance nature of the friction-based energy dissipation devices used in this study. The results shown in Fig. 6 confirm that all systems are appropriately tuned for the specified ductility factor and are ready for dynamic analysis.

The red lines in Fig. 6 represent the SLS1-level loads calculated using the force-based design method outlined in the standard (e.g., the Equivalent Static Method described in NZS 1170.5 [37]). According to the requirements of this standard, structures with importance levels of 2 and 3—such as normal buildings (IL2) and important buildings (IL3)—must satisfy serviceability requirements. These include demonstrating linear-elastic performance up to the calculated SLS1 base shear and maintaining inter-storey drifts below 0.33 %. Meeting these conditions ensures that buildings can continue functioning after small to moderate earthquakes.

As shown in Fig. 6, all nine systems satisfied this requirement. In other words, all systems exhibited linear-elastic behaviour up to and even beyond the SLS1 limit. This confirms that any yielding in the system (e.g., slip in the friction devices) only occurs at base shear levels exceeding the SLS1 threshold. The relationship between the estimated base shears in the 6-storey and twelve-storey frames highlights key characteristics of how structures respond to seismic forces at different limit states and periods. At SLS1, where no ductility is considered ($\mu=1$), the twelve-storey frame experiences higher base shears of approximately 461 kN at a lateral displacement of 71 mm, 910 kN at 116 mm, and 725 kN at 126 mm for the R3, S3, and D3 frames, respectively. In contrast, the 6-storey frames exhibit base shear forces of 467 kN at 28 mm, 940 kN at 49 mm, and 714 kN at 39 mm for the R2, S2, and D2 frames. Despite the twelve-storey frame having a longer period of 1.159 s compared to the 6-storey frame's 0.515 s, the base shear figures are close. However, the lateral elastic displacements are significantly larger in the twelve-storey frame. This difference is primarily attributed to the increased flexibility of the twelve-storey frame, resulting in a longer period, whereas the stiffer 6-storey frames exhibit significantly smaller deflections. At the Ultimate Limit State (ULS), the base shears are similar for both structures. The reduction in base shear has a more pronounced effect on the twelve-storey structures, as the longer period (1.159 s) naturally attracts lower seismic forces. When combined with a ductile response, this re-

Table 2
Frame section sizes (dimensions in mm and grades in MPa).

R1, s1, D1	Level,i	Member Section Size		
		Column	Beam	Brace
	Level 1	400 × 400-GL12	750 × 400-GL12	300 × 300-GL8
	Level 2	400 × 400-GL12	750 × 400-GL12	300 × 300-GL8
R2, S2, D2	Level,i	Member Section Size		
		Column	Beam	Brace
	Level 1	550 × 550-GL12	750 × 400-GL12	400 × 400-GL10
	Level 2	550 × 550-GL12	750 × 400-GL12	400 × 400-GL10
	Level 3	550 × 550-GL12	750 × 400-GL12	400 × 400-GL10
	Level 4	400 × 400-GL12	750 × 400-GL12	350 × 350-GL10
	Level 5	400 × 400-GL12	750 × 400-GL12	350 × 350-GL10
	Level 6	400 × 400-GL12	750 × 400-GL12	350 × 350-GL10
R3, S3, D3	Level,i	Member Section Size		
		Column	Beam	Brace
	Level 1	750 × 750-GL12	750 × 400-GL12	400 × 400-GL12
	Level 2	750 × 750-GL12	750 × 400-GL12	400 × 400-GL12
	Level 3	650 × 650-GL12	750 × 400-GL12	400 × 400-GL12
	Level 4	650 × 650-GL12	750 × 400-GL12	400 × 400-GL12
	Level 5	650 × 650-GL12	750 × 400-GL12	400 × 400-GL12
	Level 6	550 × 550-GL12	750 × 400-GL12	400 × 400-GL12
	Level 7	550 × 550-GL12	750 × 400-GL12	400 × 400-GL10
	Level 8	550 × 550-GL12	750 × 400-GL12	400 × 400-GL10
	Level 9	400 × 400-GL12	750 × 400-GL12	400 × 400-GL10
	Level 10	400 × 400-GL12	750 × 400-GL12	350 × 350-GL10
	Level 11	400 × 400-GL12	750 × 400-GL12	350 × 350-GL10
	Level 12	400 × 400-GL12	750 × 400-GL12	350 × 350-GL10

Table 3
Specifications of the friction braces.

R1	Level,i	Device Capacity (Fult)-kN	S1	Level,i	Device Capacity (Fslip)-kN	D1	Level,i	Device Capacity (Fslip)-kN
	Level 1	400		Level 1	400		Level 1	300
	Level 2	200		Level 2	200		Level 2	150
R2	Level,i	Device Capacity (Fult)-kN	S2	Level,i	Device Capacity (Fult)-kN	D2	Level,i	Device Capacity (Fult)-kN
	Level 1	1050		Level 1	1050		Level 1	790
	Level 2	940		Level 2	940		Level 2	700
	Level 3	700		Level 3	700		Level 3	525
	Level 4	700		Level 4	700		Level 4	525
	Level 5	470		Level 5	470		Level 5	350
	Level 6	235		Level 6	235		Level 6	175
R3	Level,i	Device Capacity (Fult)-kN	S3	Level,i	Device Capacity (Fslip)-kN	D3	Level,i	Device Capacity (Fslip)-kN
	Level 1	1050		Level 1	1050		Level 1	790
	Level 2	940		Level 2	940		Level 2	700
	Level 3	940		Level 3	940		Level 3	700
	Level 4	700		Level 4	700		Level 4	525
	Level 5	700		Level 5	700		Level 5	525
	Level 6	700		Level 6	700		Level 6	525
	Level 7	700		Level 7	700		Level 7	525
	Level 8	470		Level 8	470		Level 8	350
	Level 9	470		Level 9	470		Level 9	350
	Level 10	350		Level 10	350		Level 10	265
	Level 11	235		Level 11	235		Level 11	175
	Level 12			Level 12			Level 12	90

sults in base shears that are similar to those of the shorter and lighter 6-storey structures. These close ULS base shear values indicate that the combination of period-dependent spectral acceleration, seismic weight, and ductility reduction factors effectively balances the seismic demands between these two differently sized structures.

In summary, when timber structures are equipped with pinching-free energy dissipative braces (e.g. slip friction connections in this case), a taller structure may exhibit similar performance to a shorter structure in terms of base shear. This can be attributed to the more flexible nature of the taller structures. While this can be beneficial in terms of reduced base shear, the response drifts should be accurately checked

to make sure the structure can still perform as per the intended design criteria.

5. Nonlinear dynamic analyses and results

A series of Nonlinear Dynamic Time-History (NLDTH) simulations were carried out on the nine building models to further examine their performance in relation to the various hysteretic responses. For each model, 11 ground motion records were selected and scaled in accordance with the target spectra and the procedure outlined in the NZS 1170.5 standard [37] and the study presented in [49]. The records are

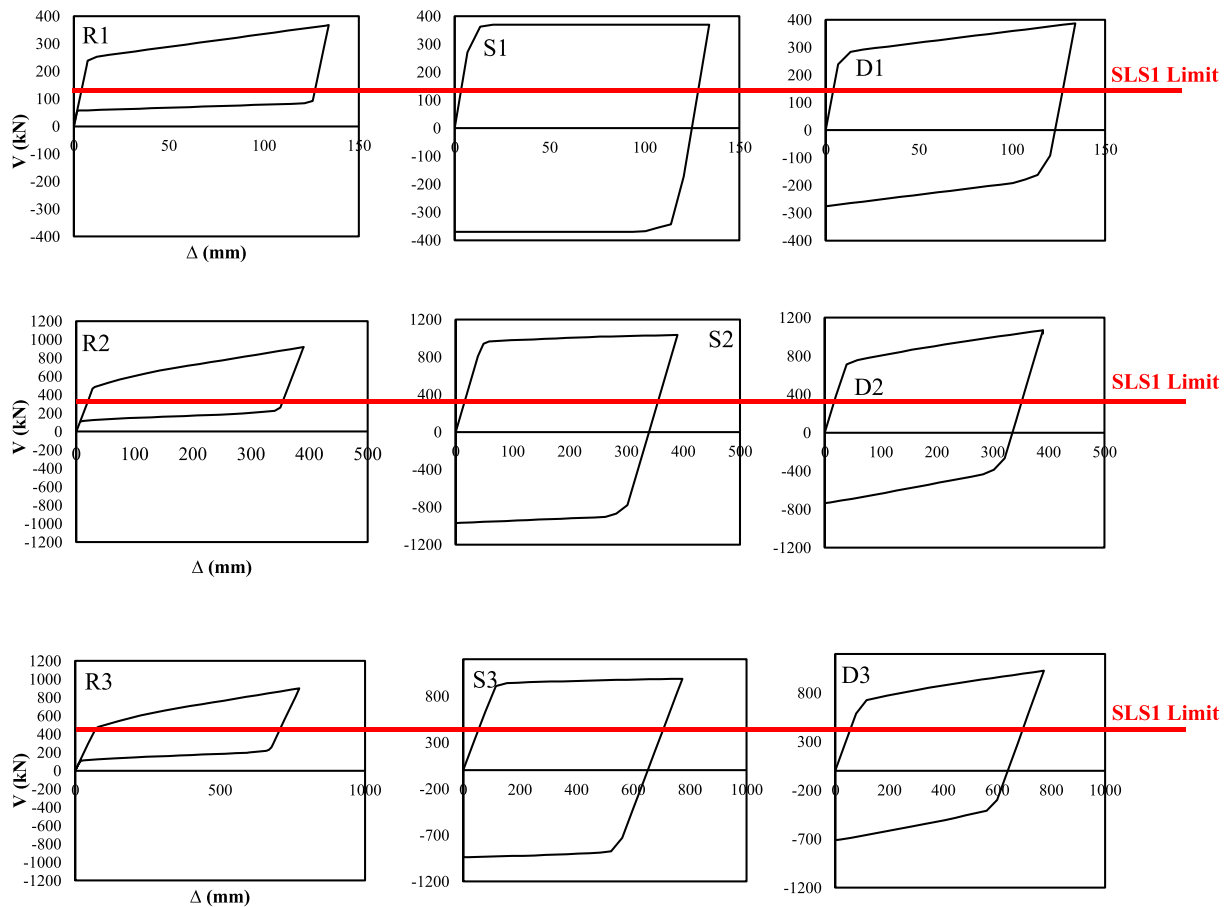


Fig. 6. Results of cyclic NSP analyses.

Table 4
Seismic events selected for the NLDTH analyses.

Event	Station	Country	Year	M _w	Fault
San Fernando	"Castaic - Old Ridge Route"	United States	1971	6.61	Reverse
Imperial Valley-06	"Brawley Airport"	United States	1979	6.53	strike slip
Livermore-02	"San Ramon - Eastman Kodak"	United States	1980	5.42	strike slip
Loma Prieta	"Hollister Differential Array"	United States	1989	6.93	Reverse Oblique
Chi-Chi_ Taiwan	"TCU101"	Taiwan	1999	7.62	Reverse Oblique
Chi-Chi_ Taiwan-03	"TCU075"	Taiwan	1999	6.2	Reverse
Taiwan SMART1(45)	"SMART1 O03"	Taiwan	1986	7.3	Reverse
L'Aquila_ Italy	"L'Aquila - V. Aterno -Colle Grilli"	Italy	2009	6.3	Normal
Chuetsu-oki_ Japan	"Joetsu Kita"	Japan	2007	6.8	Reverse
Chuetsu-oki_ Japan	"Joetsu Yasuzukaku Yasuzuka"	Japan	2007	6.8	Reverse
Iwate_ Japan	"Iwadeyama"	Iwate Japan – Japan	2008	6.9	Reverse

specifically chosen to meet the criteria in NZS1170.5 to ensure suitability in reproducing the target scaling spectra. Table 4 outlines the characteristics of the ground motions, while Fig. 7 illustrates a comparison between the target spectrum and the scaled records for two of the models (R1 and D3) as representatives for all.

Fig. 8 shows the results of the NLDTH simulations for the two-storey frames (R1, S1, and D1). In Fig. 8(a), for the R1 system, the average recorded base shear from all ground motion records is 327 kN. The highest recorded base shear is for the IWATE event at 366 kN, while the lowest is for the CHICHI event at 249 kN. These results are consistent with the base shear obtained from the nonlinear pushover analyses, which was 367 kN. While not the responses from all records match with the NSP analysis results, however, the overall behaviour of the system is well captured. For the S1 system, the average recorded base shear is 384 kN, with the IWATE event producing the highest base shear at

397 kN and the CHICHI event the lowest. Despite having a higher hysteretic damping ratio, the base shears for the S1 system are generally higher than those for the R1 system (self-centring). Note that the damping ratio discussed here refers to the area enclosed by the hysteretic loops as per the method in [23]. The D1 system, on the other hand, has an average base shear of 319 kN, closely matching the response of the R1 model. This highlights the benefits of having a positive post-slip stiffness, as seen in both the R1 and D1 systems, in controlling base shear and drift.

Fig. 8(b) illustrates the inter-storey drift responses of the R1, S1, and D1 models. The average inter-storey drift for the R1, S1, and D1 systems is 1.4 %, 0.6 %, and 0.9 %, respectively. The D1 system, which incorporates SFBFs, exhibits the lowest drifts, while the R1 and S1 systems, with positive post-slip stiffness, show slightly higher drifts. However, the drifts in all three systems remain within the max-

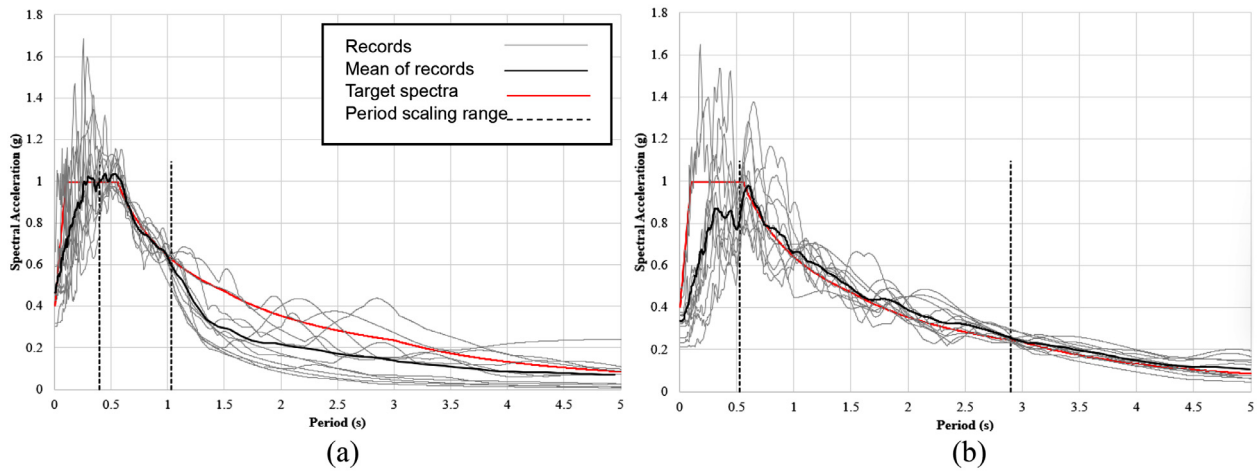


Fig. 7. Ground motions spectra and scaling: (a) R1 (b) D3.

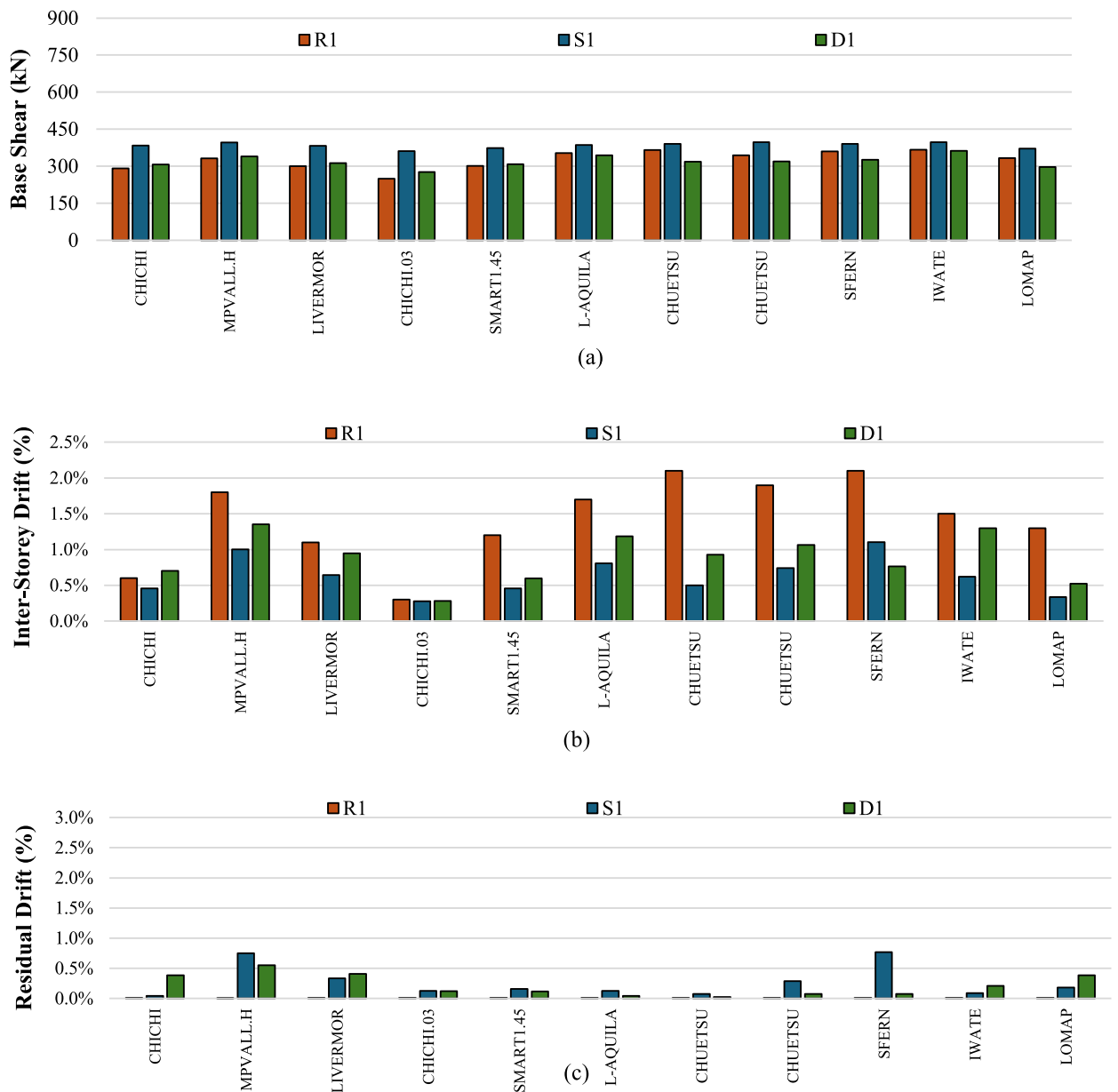


Fig. 8. NLDTH results for the two-story frames: (a) base shears (b) maximum inter-story drifts (c) residual displacements.

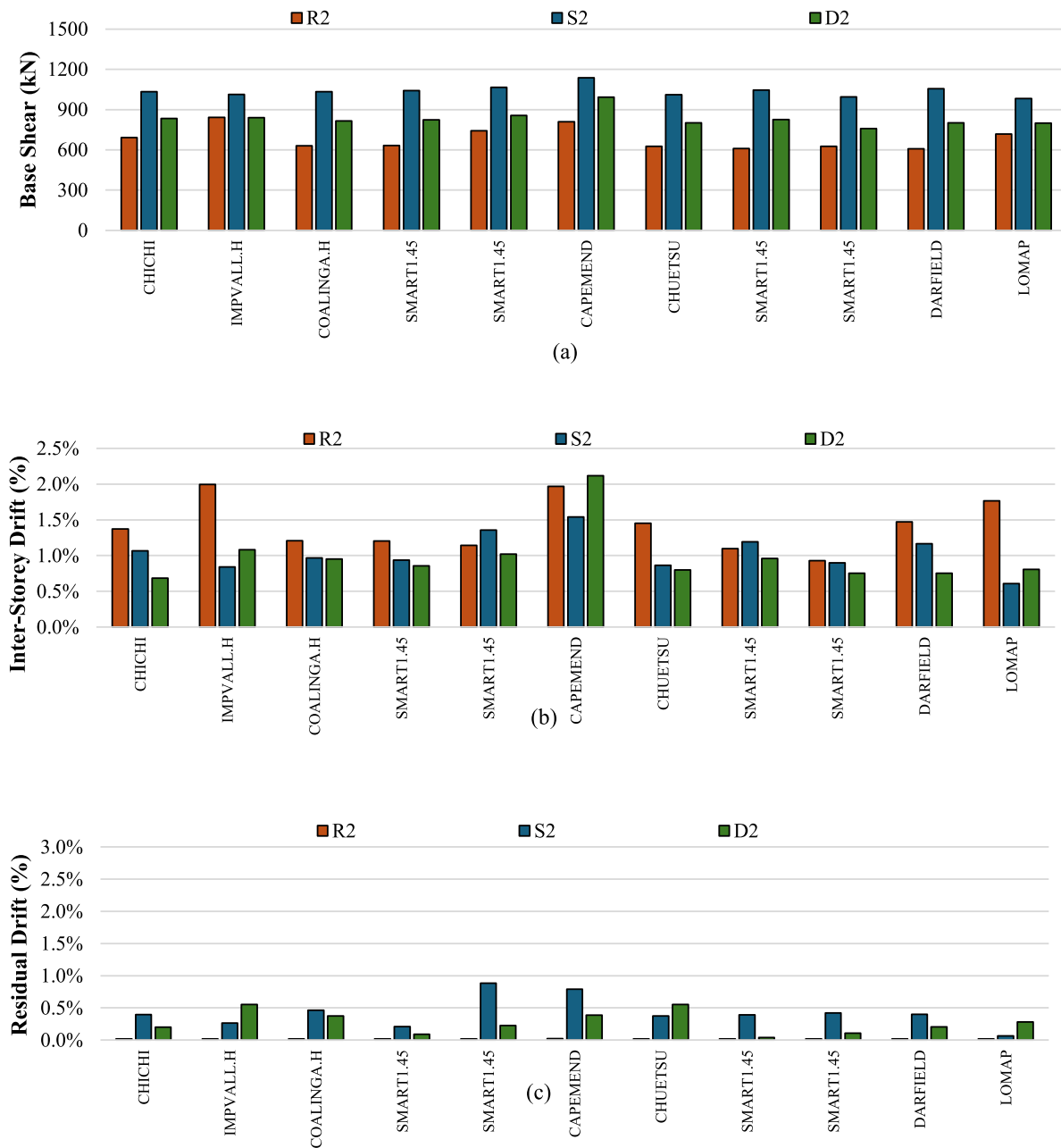


Fig. 9. NLDTH results for the six-story frames: (a) base shears (b) maximum inter-story drifts (c) residual displacements.

imum allowable inter-storey drift specified by the standard (2.5 %) and are also below the recommended limit for low-damage design [27] (approximately 1.5 %).

Fig. 8(c) presents the residual displacements for all records. Note that the residual displacement means the deformation recorded at the end of the events when the motions have ceased. As expected, the R1 model, which utilises RSFJ devices, achieves a fully self-centring behaviour with no residual displacements. This performance is due to the inherent self-centring capability of the RSFJs. Conversely, the S1 model, which behaves similarly to an E-P-P system due to the use of SFBFs, exhibits the highest recorded residual displacements. For instance, the MPVALL and L-AQUILA events result in residual drifts of 1.4 % and 1.2 %, respectively. According to the literature, residual displacements exceeding 0.5 % may significantly increase the risk of demolition. The average residual drift for the S1 system is 0.3 %. Although the S1 system demon-

strates the lowest response drifts among the three systems, it poses the highest risk of residual displacements leading to possible demolition.

The D1 model, which incorporates a dual system, has an average residual drift of approximately 0.2 %. While this is significantly lower than the S1 system, it does not achieve fully self-centring performance, as seen in the R1 system. The lower residual displacement in the D1 model compared to the S1 model is attributed to the supplementary moment-resisting frame (MRF), which works in parallel with the friction device and provides a positive post-slip stiffness. This behaviour aligns with the pushover performance of the D1 system shown in Fig. 6.

Fig. 9 shows the results for the six-storey frames (R2, S2, and D2). As observed in Fig. 9(a), the average base shear recorded across all analysed cases for the R2 system is 685 kN, with the maximum figure recorded for the IMPVALL event (843 kN) and the minimum value recorded for the DARFIELD event (608 kN). It is apparent that the base shear values are

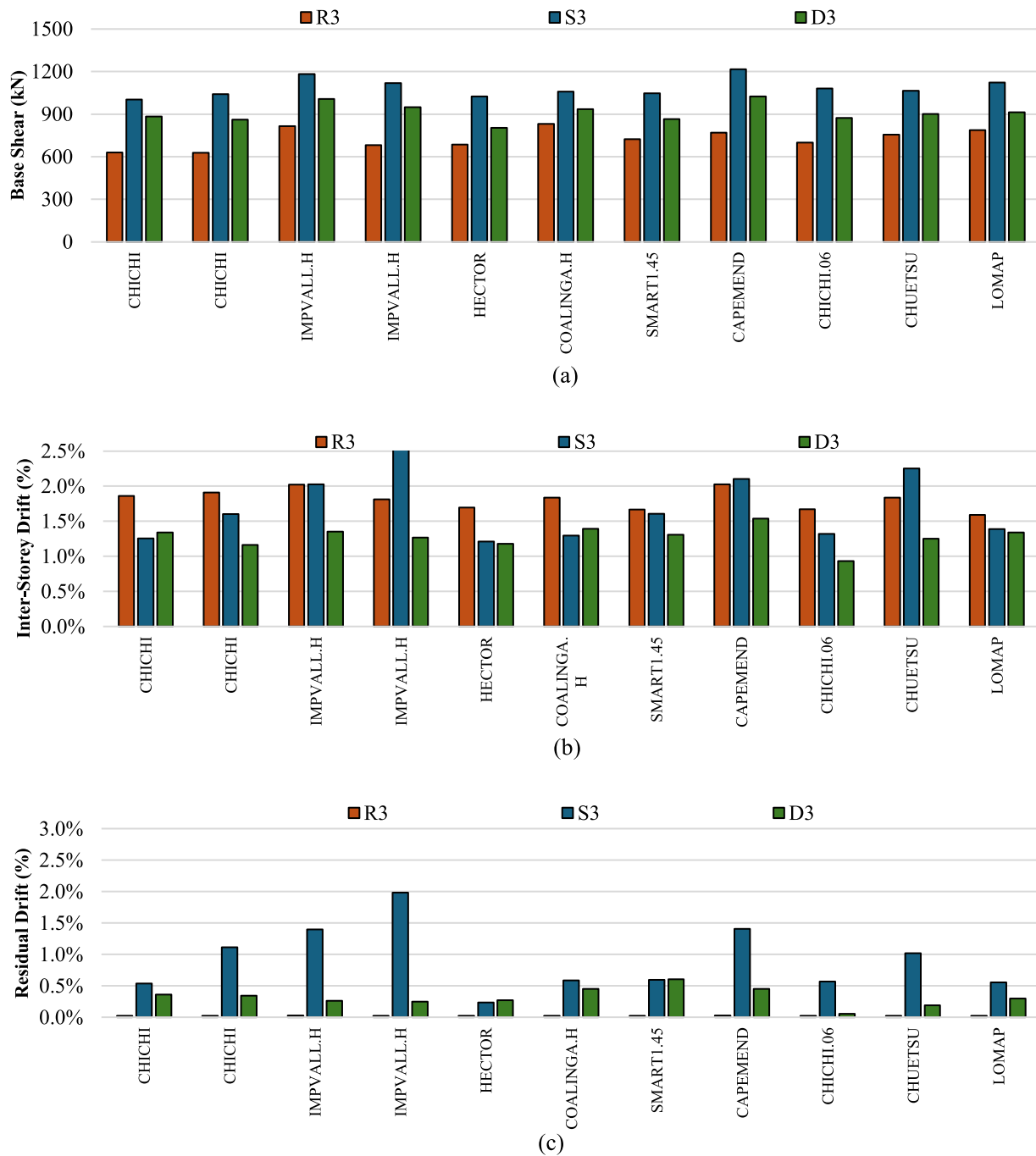


Fig. 10. NLDTH results for the 12-story frames: (a) base shears (b) maximum inter-storey drifts (c) residual displacements.

all below the base shear achieved through the NSP analysis (see Fig. 6), which is 917 kN. This indicates that the NSP exercise in this instance has been slightly conservative but still within range and well correlated with the NLDTH results.

The base shear for the S2 model is generally higher than that of the R2 model. This indicates that, despite the larger area covered by the hysteretic loop of the R2 model compared to S2 (Fig. 6), the post-slip stiffness of the RSFJ has been effective in controlling the base shear. Moreover, the base shears from the D2 model (the model with the dual system), while higher than R2, are smaller compared to the values from the S2 model. This highlights the significant contribution of having a non-zero post-slip (e.g., post-yield) stiffness in controlling the performance of the structure under earthquakes [35].

Fig. 9(b) shows the response drifts for the R2, S2, and D2 systems. The R2 system demonstrated the largest values with an average of 1.4%, while the average for the S2 and D2 systems was 1.0% in both cases. This is likely a result of the higher hysteretic damping ratio of the S2 and D2 systems compared to the R2 model. Nevertheless, even the drifts for the R2 model are significantly lower than the code-prescribed value of 2.5% or the threshold recommended for achieving a low-damage design (1.5%).

Fig. 9(c) shows the residual displacements for the three investigated systems. The R2 system demonstrated fully self-centring behaviour with no residual drifts. Similar to the two-storey frames, this can be attributed to the flag-shaped response of the RSFJs. As expected, the S2 system, which behaves like an E-P-P system, exhibited the highest residual drifts,

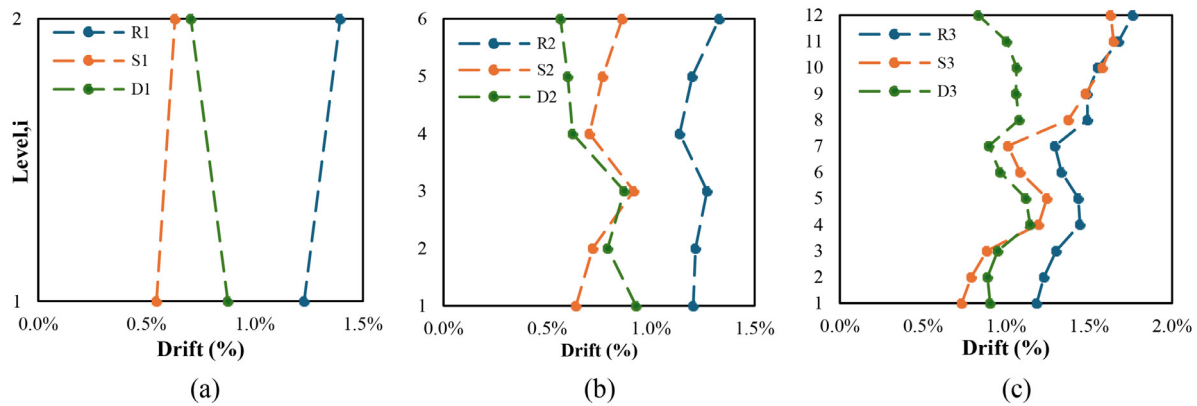


Fig. 11. Lateral drift profile of the twelve-story frames (a) two-story models (b) six-story frames (c) twelve-story frames.

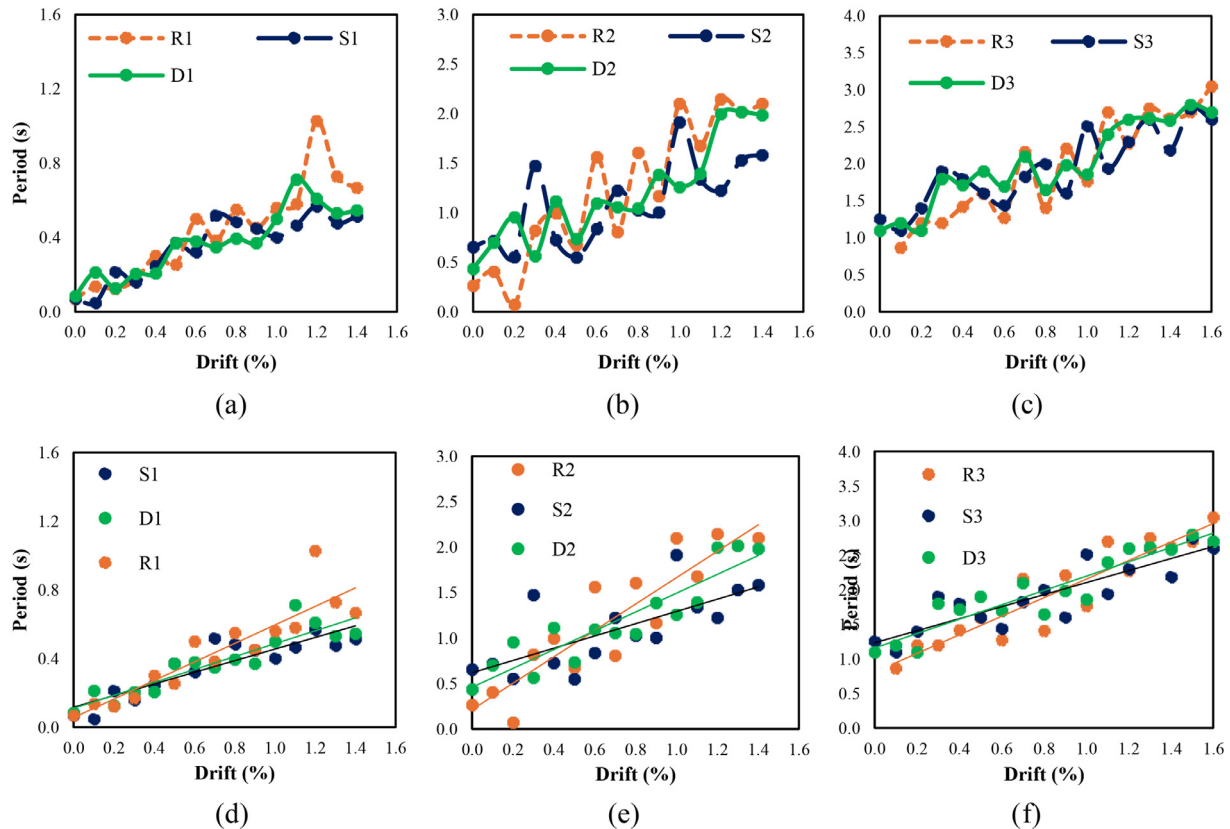


Fig. 12. Drift and period relationships: (a) two-story models (b) six-story frames (c) twelve-story frames (d) linear interpolation for two-story models (e) linear interpolation for six-story frames (f) linear interpolation for twelve-story frames.

with two instances exceeding 0.5 %. For the D2 model, the maximum recorded residual drift exceeded 0.5 % in only one case (the MPVALL event).

In general, when comparing the response of the six-storey frames with the two-storey frames, it can be observed that the response drifts are higher, while residual drifts are relatively lower. This again demonstrates that the significance of the post-slip stiffness increases as the structure becomes taller (e.g., when the structure is more flexible).

Fig. 10 shows the results of the NLDTH simulations on the twelve-storey models. As seen in Fig. 10(a), the average base shear responses for the R3, S3, and D3 models are 728 kN, 1087 kN, and 911 kN, respectively. A pattern similar to the six-storey models is observable. In other words, the models with non-zero post-slip stiffness (R3 and D3) performed better in terms of base shear control compared to the model

with an E-P-P load-deformation response (S3). However, the base shears in this instance are very close to, or in some cases even above, the base shear achieved by the NSP exercise (see the third row of figures in Fig. 6). This indicates that the NSP may be less reliable for taller structures that are more flexible.

Fig. 10(b) shows the response drifts. The average recorded lateral drifts for the R3, S3, and D3 models are 1.8 %, 1.7 %, and 1.3 %, respectively. It can be seen that similar to the base shear responses, the three models demonstrated a closer relationship compared to the two-storey and six-storey models. Additionally, the mean drift values are notably higher than those of the two-storey and six-storey models. This suggests that as the structure becomes taller and more flexible, the significance of post-slip stiffness in governing the overall seismic performance of the building diminishes.

Fig. 10(c) shows the recorded residual drifts. As expected, the S3 system demonstrated the highest residual drifts, reaching 2.0 % in one instance (IMPVALL). The R3 system exhibited a fully self-centring behaviour, as anticipated. The D3 system displayed a semi-self-centring behaviour, with residual drifts exceeding the 0.5 % threshold indicated in the literature in only one instance.

Fig. 11 shows the lateral displacement profiles for the three groups (two-, six-, and twelve-storey models), where the average recorded inter-storey drifts are plotted for each storey. As shown in Fig. 11(a), all three two-storey models performed as expected, with drifts remaining below the 1.5 % threshold for low-damage design. The lateral displacement profiles of the R2, S2, and D2 systems are illustrated in Fig. 11(b). It can be observed that all systems exhibited similar behaviour, with the R2 system showing slightly higher response drifts. Nevertheless, the response drifts for all three systems remain well below the 1.5 % low-damage design threshold. Fig. 11(c) presents a similar pattern for the R3, S3, and D3 systems. However, the displacement profiles of these three systems are relatively lower compared to the data shown in Fig. 11(b). This indicates that as the structure becomes taller and more flexible, all friction-based systems begin to exhibit more similar behaviour.

Fig. 12 exhibits a comparison of drift and period relationships across different building heights that reveals fundamental aspects of structural dynamic behaviour [50]. As inter-story drifts increase, the structures exhibit increased flexibility, which directly influences the fundamental periods. It is evident that the initial periods at zero drift represent the structure's elastic behaviour, while period elongation at higher drift levels indicates increased structural flexibility. For instance, in the 2-story structure, the period increases from 0.1 s at negligible drift to 0.7 s at 1.4 % drift, demonstrating how drift-induced flexibility lengthens the vibration period. This means when energy dissipation is utilised, the effective stiffness of the structure reduces, and the effective drifts increase. This effect becomes more pronounced in taller structures, with the 6-story building showing period elongation from 0.3 s to 2.1 s, and the 12-story structure exhibiting an increase from 0.3 s to 2.4 s at maximum drift levels.

Moreover, the progressive increase in period with drift indicates softening of the structural system, where larger deformations lead to reduction in effective stiffness and consequently, longer vibration periods. This phenomenon is particularly important for seismic design as longer periods generally result in different seismic force distributions and can influence the structure's response to earthquake excitations.

Overall, this study for the first time made a direct comparison to better understand seismic performance of mass timber frames with different types of friction-damped braces. It compared the most important performance indexes (hysteresis, base shear drifts and residual displacements) and recommendations are made. Note that the base of the structure is considered as rigid. The results of the NLDTH simulations demonstrated that all three friction-based lateral load-resisting systems for mass timber structures, as detailed in Table 1, can perform as expected according to the loading standards. However, if performance levels beyond life safety (the minimum code requirement) are targeted, self-centring systems may be the preferred option. Although mass timber systems designed with conventional friction-damped braces performed well in terms of base shear reduction and response inter-storey drifts, they exhibited significant residual displacements in some cases, which can be an undesirable outcome for resilient seismic design. The study also highlighted that dual systems, comprising conventional friction-damped timber braces and a backup moment-resisting frame, can be a viable solution to minimise residual displacements while satisfying code requirements.

6. Conclusions

This paper investigated the seismic behaviour of mass timber systems equipped with three different forms of lateral load-resisting systems incorporating friction-damped braced frames. A fully self-centring system,

a fully elastic-perfectly-plastic (E-P-P) system, and a semi-self-centring system were studied. To understand the effect of building height, period, and lateral flexibility on the overall seismic performance of these building types, three different models for two-, six-, and twelve-storey frames were developed and analysed. Nonlinear static pushover analyses, followed by nonlinear dynamic simulations, were conducted to extract critical seismic performance data.

From the numerical results, it can be concluded that all three systems performed well in terms of response drifts and base shear control. In other words, the base shear and drifts associated with all three building systems were within the code-allowed limits. Furthermore, it was demonstrated that using conventional sliding friction-damped braces as the sole lateral load-resisting mechanism may result in significant residual displacements, potentially compromising the post-earthquake performance of the building. In this regard, it is recommended to use either Resilient Slip Friction Joint (RSFJ) braces or conventional friction-damped braces parallel to a backup moment-resisting frame to improve performance and minimise residual displacements. Additionally, it was shown that as buildings increase in height and become more flexible, the differences in hysteretic behaviour (e.g., load-deformation response) between the systems become less apparent and less significant. Therefore, the use of E-P-P systems may be more feasible for taller buildings.

In summary, friction-damped braced frames can be considered a viable and potentially economical solution for implementing mass timber frames in seismically active regions such as New Zealand. Future studies could investigate the response accelerations of friction-damped mass timber frames compared to conventional timber braces. Furthermore, the applicability of the concepts developed in this paper for post-disaster buildings could be explored. Furthermore, proposing simplified methods for estimating seismic actions based on fundamental periods, drift considerations and brace characteristics will be considered.

Relevance to resilience

An efficient way to introduce seismic resilience into multi-storey mass timber structures is through the use of sliding friction connections as braces. This paper investigates the seismic performance of such structures when equipped with either conventional or self-centring slip friction connections. The findings provide readers with valuable insight into the advantages and limitations of each bracing system, enabling more informed design decisions for resilient timber buildings. This work contributes to improving the seismic resilience of timber construction by introducing innovative and modern connection technologies.

Declaration of competing interest

The authors declare that they have no known competing financial interests or personal relationships that could have appeared to influence the work reported in this paper.

CRediT authorship contribution statement

Ashkan Hashemi: Writing – review & editing, Writing – original draft, Supervision, Project administration, Methodology, Investigation, Formal analysis, Conceptualization. **Rajnil Lal:** Validation, Methodology, Investigation, Formal analysis.

Acknowledgement

This research received no specific grant from any funding agency in the public, commercial, or not-for-profit sectors.

References

- [1] Junda E, Málaga-Chuquitaype C. Life cycle impacts of structural deterioration and seismic events on cross-laminated timber buildings. *J Build Eng* 2025;104:112282.

- [2] Salgado RA, Guner S. A structural performance-based environmental impact assessment framework for natural hazard loads. *J Build Eng* 2021;43:102908.
- [3] P. Quenneville, A. Hashemi, and P. Zarnani, "Traditional seismic fuses in timber structures - pros and cons," 2025.
- [4] Demirci C, Málaga-Chuquitaype C, Macorini L. Seismic drift demands in multi-storey cross-laminated timber buildings. *Earthq Eng Struct Dyn* 2018;47(4):1014–31.
- [5] Sustersic I, Fragiaco M, Dujic B. Seismic analysis of cross-laminated multistory timber buildings using code-prescribed methods: influence of panel size, connection ductility, and schematization. *J Struct Eng* 2016;142(4) E4015012.
- [6] Ceccotti A, Sandhaas C, Okabe M, Yasumura M, Minowa C, Kawai N. SOFIE project-3D shaking table test on a seven storey full scale cross laminated timber building. *Earthq Eng Struct Dyn* 2013;42(13):2003–21.
- [7] Chen Z, Popovski M. Seismic response of braced heavy timber frames with riveted connections. *J Perform Constr Facil* 2021;35(5):4021051.
- [8] M. Popovski and E. Karacabeyli, "Seismic behaviour of cross-laminated timber structures," 2012.
- [9] Gavric I, Fragiaco M, Ceccotti A. Cyclic behavior of CLT wall systems: experimental tests and analytical prediction models. *J Struct Eng* 2015;141(11):4015034.
- [10] Popovski M, Gavric I. Performance of a 2-story CLT house subjected to lateral loads. *J Struct Eng* 2015 E4015006.
- [11] Yasumura M, Kobayashi K, Okabe M, Miyake T, Matsumoto K. Full-scale tests and numerical analysis of low-rise CLT structures under lateral loading. *J Struct Eng* 2015 E4015007.
- [12] Lal R, Hashemi A, Quenneville P. An innovative connection system for platform-type mass timber buildings. *Resilient Cities Struct* 2025;4(2):14–29.
- [13] Yan L, Li Y, Chang W-S, Huang H. Seismic control of cross laminated timber (CLT) structure with shape memory alloy-based semi-active tuned mass damper (SMA-STMD). *Structures* 2023;57:105093.
- [14] Badal PS, Tesfamariam S. Seismic collapse performance of high-rise mass timber building with buckling-restrained braced frames. *Soil Dyn Earthq Eng* 2024;177:108369.
- [15] Daneshvar H, Chui YH, Dickof C, Tannert T. Experimental parametric study of perforated steel plate fuses for mass timber seismic force resisting systems. *J Build Eng* 2023;73:106772.
- [16] Chen F, Li M, He M, Li Z. Direct displacement-based design and seismic performance evaluation of post-tensioned steel-timber hybrid frames equipped with braces. *J Build Eng* 2025;99:111660.
- [17] Pall AS, Marsh C. Response of friction damped braced frames. *J Struct Eng* 1982;108(9):1313–23.
- [18] Baktash P, Marsh C, Pall A. Seismic tests on a model shear wall with friction joints. *Can J Civ Eng* 1983;10(1):52–9.
- [19] Popov EP, Grigorian CE, Yang T-S. Developments in seismic structural analysis and design. *Eng Struct* 1995;17(3):187–97.
- [20] Filiatraut A, Cherry S. Seismic design spectra for friction-damped structures. *J Struct Eng* 1990;116(5):1334–55.
- [21] Loo WY, Kun C, Quenneville P, Chow N. Experimental testing of a rocking timber shear wall with slip-friction connectors. *Earthq Eng Struct Dyn* 2014;43(11):1621–39.
- [22] Dal Lago B, Biondini F, Toniolo G. Friction-based dissipative devices for precast concrete panels. *Eng Struct* 2017;147:356–71. doi:10.1016/j.engstruct.2017.05.050.
- [23] Priestley MJKMJN, Calvi GM. Displacement-Based seismic design of structures. Pavia, Italy: IUSS Press; 2007.
- [24] Ramirez CM, Miranda E. Significance of residual drifts in building earthquake loss estimation. *Earthq Eng Struct Dyn* 2012;41(11):1477–93 Sep. doi:10.1002/eqe.2217.
- [25] J. McCormick, H. Aburano, M. Ikenaga, and M. Nakashima, "Permissible residual deformation levels for building structures considering both safety and human elements," in *Proceedings of the 14th world conference on earthquake engineering*, 2008, pp. 12–17.
- [26] Upadhyay A, Pantelides CP, Ibarra L. Residual drift mitigation for bridges retrofitted with buckling restrained braces or self centering energy dissipation devices. *Eng Struct* 2019;199:109663.
- [27] Bruneau M, MacRae G. Building structural systems in Christchurch's Post-earthquake reconstruction. *Earthq Spectra* 2019;35(4):1953–78.
- [28] Hashemi A, Zarnani P, Masoudnia R, Quenneville P. Seismic resistant rocking coupled walls with innovative resilient Slip friction (RSF) joints. *J Constr Steel Res* 2017;129:215–26.
- [29] Bagheri H, Hashemi A, Zarnani P, Quenneville P. The resilient slip friction joint tension-only brace beyond its ultimate level. *J Constr Steel Res* 2020;172:106225.
- [30] Hashemi A, et al. Enhanced seismic performance of timber structures using resilient connections: full-scale testing and design procedure. *J Struct Eng* 2020;146(9):04020180.
- [31] Yousef-Beik SMM, Veismoradi S, Zarnani P, Hashemi A, Quenneville P. Experimental study on cyclic performance of a damage-free brace with self-centering connection. *J Struct Eng (United States)* 2021;147(1). doi:10.1061/(ASCE)ST.1943-541X.0002869.
- [32] Bagheri H, Hashemi A, Yousef-Beik SMM, Zarnani P, Quenneville P. New self-centering tension-only brace using resilient slip-friction joint: experimental tests and numerical analysis. *J Struct Eng* 2020;146(10) 04020219–18.
- [33] A. Hashemi, P. Zarnani, P. Quenneville, C. Wallington, D. Whittaker, and S. Govind, "Lincoln University Waimarie building: an application of friction damping devices with recentering for low damage design," 2023.
- [34] A. Hashemi, P. Quenneville, I. Prionas, A. Sayadi, and P. Zarnani, "Application of low damage tension braces in top extensions of existing buildings: a case study for seismic upgrade," 2024.
- [35] Hashemi A, Zarnani P, Quenneville P. Seismic assessment of rocking timber walls with energy dissipation devices. *Eng Struct* 2020;221:111053.
- [36] American Society of Civil Engineers, "ASCE/SEI standard 7-16. Minimum design loads and associated criteria for buildings and other structures," 2016.
- [37] New Zealand Standards, "Structural design actions (NZS 1170.5)," Wellington, New Zealand, 2004.
- [38] C. and Structures, "SAP2000 Ver. 24 (2023)." Berkeley, CA, 2023.
- [39] Hashemi A, et al. Seismic performance of a damage avoidance self-centering brace with collapse prevention mechanism. *J Constr Steel Res* 2019;155:273–85.
- [40] Hashemi A, Quenneville P. Large-scale testing of low damage rocking Cross Laminated Timber (CLT) wall panels with friction dampers. *Eng Struct* 2020;206:110166.
- [41] Hashemi A, Clifton GC, Bagheri H, Zarnani P, Quenneville P. Proposed design procedure for steel self-centering tension-only braces with resilient connections. *Structures* 2020;25:147–56 January. doi:10.1016/j.istruc.2020.02.024.
- [42] Hashemi A, Bagheri H, Zarnani P, Quenneville P. Seismic performance of friction-damped steel frames integrated with resilient tension-only braces. *J Constr Steel Res* 2021;176. doi:10.1016/j.jcsr.2020.106381.
- [43] Hashemi A, Masoudnia R, Quenneville P. Seismic performance of hybrid self-centering steel-timber rocking core walls with slip friction connections. *J Constr Steel Res* 2016;126:201–13. doi:10.1016/j.jcsr.2016.07.022.
- [44] S. Varier, A. Hashemi, P. Zarnani, and P. Quenneville, "Improved seismic performance of timber braced frame structures using resilient slip friction joint mechanism: a comparative design case study," 2020.
- [45] Hashemi A, Masoudnia R, Quenneville P. A numerical study of coupled timber walls with slip friction damping devices. *Constr Build Mater* 2016;121:373–85.
- [46] Hashemi A, Zarnani P, Masoudnia R, Quenneville P. Seismic resilient lateral load resisting system for timber structures. *Constr Build Mater* 2017;149. doi:10.1016/j.conbuildmat.2017.05.112.
- [47] Hashemi A, Zarnani P, Masoudnia R, Quenneville P. Seismic resistant rocking coupled walls with innovative resilient Slip friction (RSF) joints. *J Constr Steel Res* 2017;129. doi:10.1016/j.jcsr.2016.11.016.
- [48] Hashemi A, Zarnani P, Masoudnia R, Quenneville P. Experimental testing of rocking Cross laminated timber (CLT) walls with resilient slip friction (RSF) joints. *J Struct Eng* 2017;144(1) 04017180–1 to 04017180–16.
- [49] Burlotos C, Walsh K, Goded T, McVerry G, Brooker N, Ingham J. Seismic zonation and default suites of ground-motion records for time-history analysis in the South Island of New Zealand. *Bull New Zeal Soc Earthq Eng* 2022;55(1):25–42.
- [50] Ditommaso R, Lamarucciola N, Ponzio FC. Prediction of the fundamental period of infilled RC framed structures considering the maximum inter-story drift at different design limit states. *Structures* 2024;63:106422.